

# Determination of the radius of curvature of the anterior lens surface from the Purkinje images

George Smith<sup>1</sup> and Leon F. Garner<sup>2</sup>

<sup>1</sup>Optical Sciences Laboratory, Department of Optometry, University of Melbourne, Australia; and <sup>2</sup>Centre for Vision Research, Department of Optometry, University of Auckland, New Zealand

## Summary

A new method for calculating the radius of curvature of the anterior surface of the crystalline lens from the measured heights of the Purkinje image PI and PIII is given. Equations are developed for determination of the radius of curvature of the equivalent mirror for three configurations commonly used in phakometry. The method can be applied to targets at any distance from the corneal vertex, for both a stationary target mounted independently of the camera, and for a mobile source attached to the camera where the distance of the target to the corneal vertex will change as the camera is refocused from image PI to PIII. The situation where only one recording is made of images PI and PIII, where the camera is focused on image PI, and the height of the defocused image of PIII is measured is also considered. The errors in calculating the anterior lens radius with the equivalent mirror method if no allowance is made for an object at a finite distance is examined. The new method described is an alternative to collimating targets to overcome the errors in phakometry that occur with targets at finite distances.

## Introduction

Although the anterior surface of the crystalline lens is not the major refracting surface of the eye, it is of interest because it is the surface that shows the greatest change during accommodation of the eye (Brown, 1973), and during the growth of the eye over the period that myopia tends to develop (Garner *et al.*, 1995; Zadnik *et al.*, 1993). The radius of curvature of the anterior lens surface is usually determined by the comparison phakometry technique, which is based on the equivalent mirror theorem. The equivalent mirror theorem states that an optical system consisting of a number of refracting surfaces followed by a reflecting surface can be replaced by a single 'equivalent mirror'. The heights of the Purkinje image PI ( $h'_1$ ) and PIII ( $h'_3$ ) formed by reflection of a target from the cornea and anterior lens surface may be measured from either a photographic or a video recording, and the radius of curvature of the equivalent mirror  $r'_3$

determined from the expression:

$$r'_3 = r_1 \left( \frac{h'_3}{h'_1} \right) \quad (1)$$

where  $r_1$  is the radius of curvature of the cornea (Bennett and Rabbetts, 1989). The equivalent mirror theorem also states that the vertex and centre of curvature of the equivalent mirror are conjugates of the vertex and centre of curvature of the real mirror, imaged by the refracting surfaces (Bennett and Rabbetts, 1989). As the radius of curvature of the cornea and the depth of the anterior chamber are usually known, and assuming a refractive index for the aqueous humour, paraxial ray tracing is all that is required to find  $r_3$ , the radius of curvature of the anterior lens surface. The method is outlined in the *Appendix*.

In terms of paraxial optics this method is quite valid; however, there are two practical difficulties that can lead to errors in the determination of  $r_3$ . Firstly, the expression above is only valid if the targets used to form the Purkinje images are at optical infinity, because for a distant object the image formed by reflection is proportional to the focal

length of the surface, which is equal to one-half of the radius of curvature of the surface (Bennett and Rabbetts, 1989). In practice, the advantages of placing the target at a finite distance in front of the eye include brighter images and ease of construction of apparatus, but use of a target at a finite distance will lead to a different image position and height than that assumed by the comparison phakometry technique. This problem has been addressed by Mutti *et al.* (1992) by using a collimating lens to place the target at infinity, and by Garner *et al.* (1995) with an optimisation procedure that did not rely on the equivalent mirror method. The second potential source of error is due to the fact that images PI, and PIII are formed in different planes. While the PI and PIV images are close, PIII formed by the anterior surface of the crystalline lens is approximately 7 mm behind the plane of PI and PIV, making it difficult to focus all three images in a single recording. The choice is usually to focus images PI and PIV and then to refocus on image PIII, or to choose an intermediate plane on which to focus the recording device. In general, the size of an image changes with the level of defocus and unless this change in size is taken into account, the defocus will lead to erroneous results. This problem can be overcome by either refocusing the camera by changing the camera distance from the eye, by using a telecentric stop (Philips *et al.*, 1988), or by calculation using the method described in Option 3 in this paper.

If the recording device is not refocused and a single record is made, either PI and PIV or PIII will be defocused leading to potential errors in the measured image height, depending on the position of the entrance pupil of the recording device. If separate records are made for PI/PIV and PIII, the height of the image will also depend on whether the target is attached to the camera (mobile source), or mounted independently (stationary source).

The purpose of this study was to develop computing schemes for calculation of the radius of curvature of the anterior lenticular surface that addresses the difficulties in using Purkinje images for that purpose. The new method avoids the need to refocus the camera, and takes into account finite targets at varying distances.

## Method

The Gullstrand–Emsley schematic eye was used in the following derivations of the equations, and although this eye is a three-surface eye, with the cornea represented as a single refracting surface, it is an appropriate model for oculometric studies as measurement of the posterior surface of the cornea is not usually made. The equations presented in the *Appendix* are well known and not newly developed, but have been included for completeness.

In general, if an object height  $h$  is placed at a distance  $l$  in front of a mirror of radius of curvature  $r$  as shown in the *Appendix* (see *Figure 5*), the image distance  $l'$  will be given by the equation:

$$l' = \frac{lr}{(2l - r)} \quad (2)$$

and the image size  $h'$  is given by the equation:

$$h' = Mh \quad (3)$$

where  $M$  is the transverse magnification given by:

$$M = -\frac{l'}{l} \quad (4)$$

Combining Equations (2) and (4) gives:

$$M = \frac{r}{(r - 2l)} \quad (5)$$

which can be expressed as:

$$r = \frac{2lM}{(M - 1)} \quad (6)$$

In the case of the Gullstrand–Emsley schematic eye, we will know the transverse magnification  $M_1$  and the image height  $h'_1$  for the corneal image PI, and image height  $h'_3$  for PIII. An equation for the transverse magnification  $M_3$  in terms of these values can be found by solving Equations (3) and (4) for two sets of images to give:

$$M_3 = M_1 \left[ \frac{h'_3}{h'_1} \right] \quad (7)$$

We now consider three options regarding the positioning of the target and the plane on which the camera is focused.

### Option 1

In this case, the distance from the target to the corneal vertex is fixed, i.e. a stationary source, and the camera is focused on image PI and then moved forward to focus on image PIII.

If the distance from the target to the corneal vertex is  $s$ , and the distance from the corneal vertex to the equivalent mirror is  $w$ , then when the camera is focused on image PI as shown in *Figure 1a*:

$$l_1 = -s \quad (8)$$

and the transverse magnification is given by:

$$M_1 = \frac{h'_1}{h_0} \quad (9)$$

and from Equation (5) we have:

$$M_1 = \frac{r_1}{(r_1 - 2l_1)} \quad (10)$$

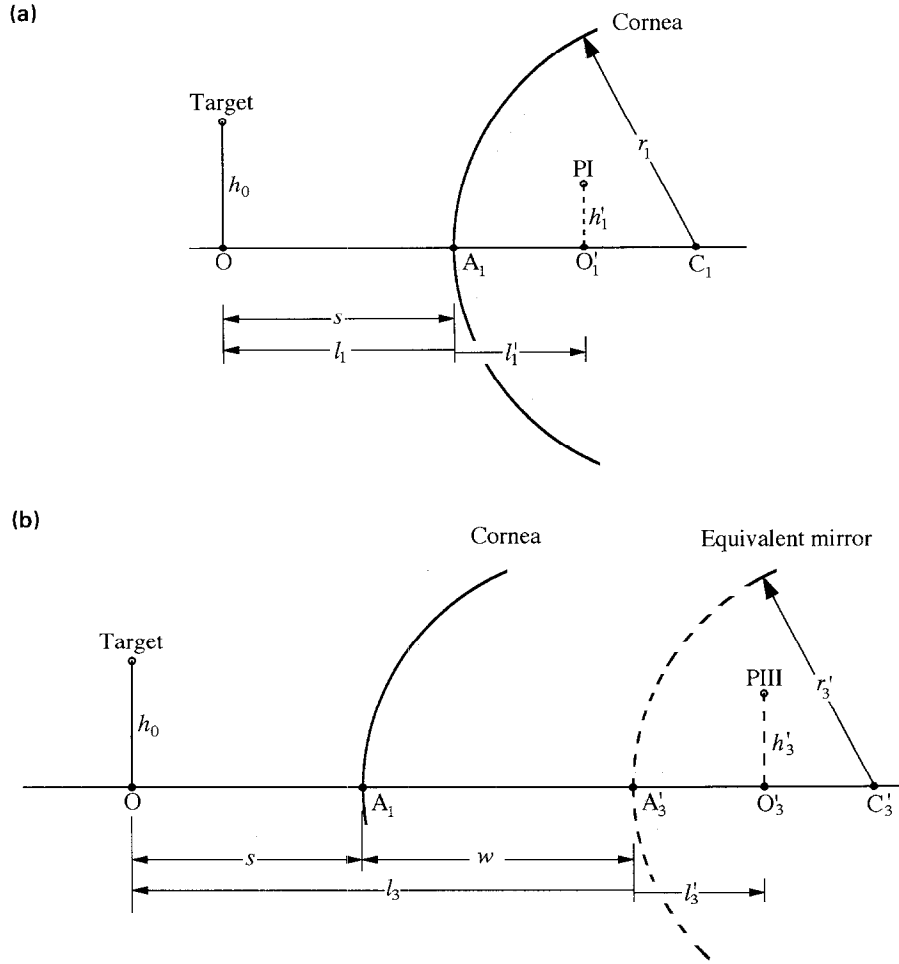


**Figure 1.** (a) The target is fixed at  $O$ , a distance  $s$  in front of the cornea, and the camera is first focused on image PI located at  $O'_1$ , and then on image PIII, located at  $O'_3$ . (b) The centre of curvature of the equivalent mirror is at  $C'_3$ .

When the camera is focused on image PIII, the situation is as shown in *Figure 1b* and:

$$l_3 = -s - w \quad (11)$$

The magnification  $M_3$  is given by:

$$M_3 = \frac{h'_3}{h_0} \quad (12)$$

and from Equations (9) and (12) we have:

$$M_3 = M_1 \left[ \frac{h'_3}{h'_1} \right] \quad (13)$$

and from Equation (5) we also have:

$$M_3 = \frac{r'_3}{(r'_3 - 2l_3)} \quad (14)$$

We can solve this equation for  $r'_3$  to obtain:

$$r'_3 = \frac{2l_3 M_3}{(M_3 - 1)} \quad (15)$$

The actual radius of curvature  $r_3$  can then be calculated using the paraxial equations contained in the *Appendix*.

#### Option 2

In this case, the target is fixed to the camera, and the camera is focused on PI and then PIII (*Figure 2*). The target moves with the camera, and hence will be a fixed distance  $t$  from the in-focus plane of the camera. As shown in *Figure 2a*, when the camera is focused on PI, this distance will be:

$$t = l'_1 - l_1 \quad (16)$$

The magnification  $M_1$  can be obtained from Equation (4) as:

$$M_1 = -\frac{l'_1}{l_1} \quad (17)$$

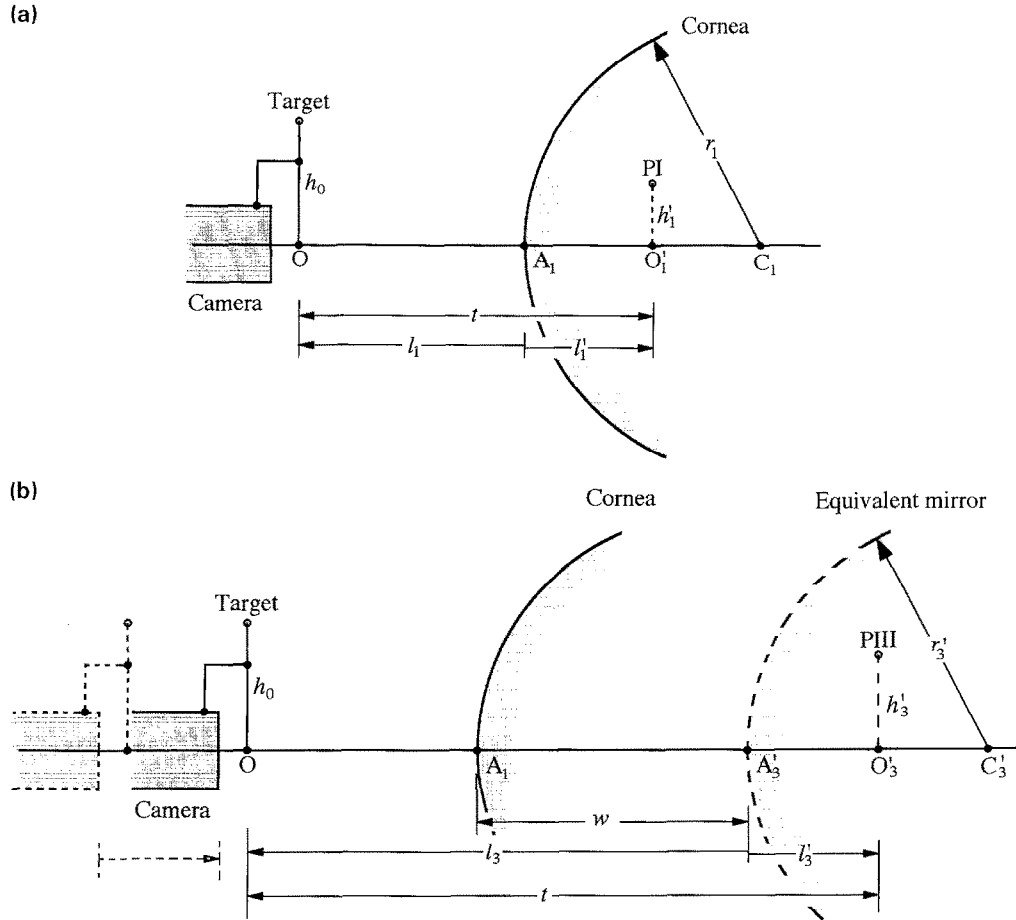


**Figure 2.** The target is fixed to the camera, and the distance  $t$  from the target to the image when focused on (a) PI and on (b) PIII will be constant. The equivalent mirror is situated a distance  $w$  from the corneal vertex.

and from Equation (5):

$$M_1 = \frac{r_1}{r_1 - 2l_1} \quad (18)$$

Solving for  $l_1$  from Equations (16), (17) and (18) gives:

$$2l_1^2 + 2(t - r_1)l_1 - r_1t = 0 \quad (19)$$

which is a quadratic equation in  $l_1$ , and can be written in the form:

$$al_1^2 + bl_1 + c = 0 \quad (20)$$

where  $a = 2$ ,  $b = 2(t - r_1)$  and  $c = -r_1t$ . This equation has two solutions:

$$l_1 = \frac{-b \pm \sqrt{b^2 - 4ac}}{2a} \quad (21)$$

Because of the sign convention, the correct value is the negative solution to Equation (21).

If the camera is now moved toward the eye to focus on image PIII, it can be seen from Figure 2b that:

$$t = l'_3 - l_3 \quad (22)$$

and from Equation (4), the transverse magnification  $M_3$  is:

$$M_3 = -\frac{l'_3}{l_3} \quad (23)$$

Solving Equations (22) and (23) gives:

$$l_3 = \frac{-t}{(1 + M_3)} \quad (24)$$

Using the value for  $l_3$  from Equation (24) and  $M_3$  from Equation (13) we can solve for  $r'_3$  using Equation (6) to give:

$$r'_3 = \frac{2l_3M_3}{(M_3 - 1)} \quad (25)$$

## Option 3

In this option, the camera is focused on image PI, and only one recording is made. Thus while the image PI will be sharp, the image PIII will be blurred, and hence may lead to a measured image height that is different from the focused image. Figure 3a shows the geometry of a camera focused in front of the image plane. The beam of light from the extreme edge of the image forms a blur disc in the plane in which the camera is focused. Figure 3a also shows that the image size  $h'_b$  measured from the centre of the defocused blur disc will be different from the actual size  $h'$ , and that the measured size will depend on the position of the aperture stop of the camera lens. Therefore in this option we must know the position of the entrance pupil of the camera.

Figure 3b shows the situation with the camera focused on PI in the plane at  $O'_1$ . The recorded size of image PIII will be the size of PIII projected on to the plane  $O'_1$  through the entrance pupil of the camera lens. From similar triangles in Figure 3b it can be seen that:

$$\frac{h'_3}{l'_3 - l_3 + b} = \frac{h'_{3b}}{l'_1 - l_1 + b} \quad (26)$$

Solving for  $h'_3$  we have:

$$h'_3 = \frac{h'_{3b}(l'_3 - l_3 + b)}{(l'_1 - l_1 + b)} \quad (27)$$

In order to calculate the value of  $h'_3$ , we need to know the values of  $h'_{3b}$ ,  $b$ ,  $l_1$ ,  $l'_1$ ,  $l_3$  and  $l'_3$ . We can measure the height  $h'_{3b}$  and in principle be able to find the value of  $b$ , the distance from the target to the entrance pupil of the camera. We can find the values  $l_1$ ,  $l'_1$  and  $l_3$  in the same manner as for Option 1, in which we have from Equation (8):

$$l_1 = -s \quad (28)$$

and the known value of  $r_1$  we can calculate the magnification  $M_1$  from Equation (10) as:

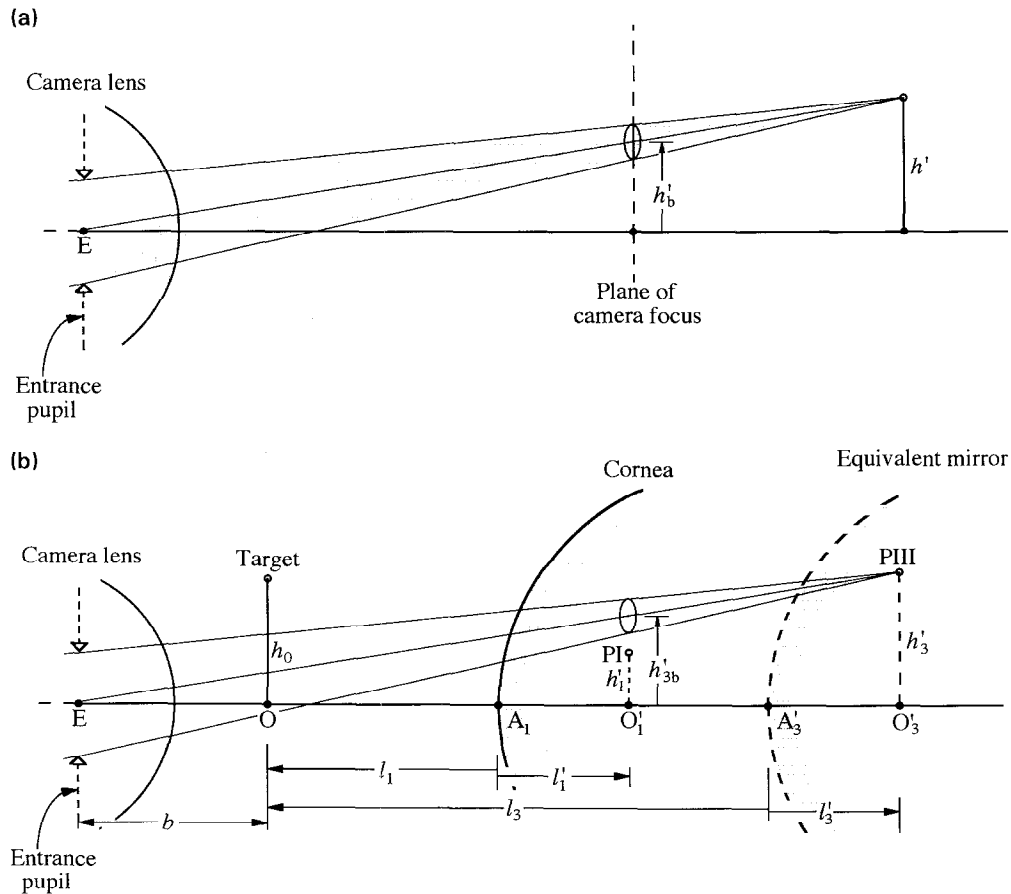


**Figure 3.** (a) The target is fixed at O, the camera is focused on image PI, and a defocused image of PIII is recorded in the plane of the camera focus (b). The height of the blurred image of PIII is  $h'_{3b}$  and is related to the actual image height  $h'_3$ .

$$M_1 = \frac{r_1}{(r_1 - 2l_1)} \quad (29)$$

From Equation (4) we now have:

$$l'_1 = -M_1 l_1 \quad (30)$$

and from Equation (11) we have:

$$l_3 = -s - w \quad (31)$$

At this stage we do not know the value of  $l'_3$  but this and the other unknowns  $h'_3$ ,  $M_3$  and  $r'_3$  are related by the following equations.

From Equation (7):

$$M_3 = M_1 \left[ \frac{h'_3}{h'_1} \right] \quad (32)$$

and from Equation (6):

$$r'_3 = \frac{2l_3 M_3}{(M_3 - 1)} \quad (33)$$

With this value of  $r'_3$ , we can find the value of  $l'_3$  from Equation (2) as:

$$l'_3 = \frac{l_3 r'_3}{2l_3 - r'_3} \quad (34)$$

These equations can be solved to give the following quadratic equation in  $r'_3$ :

$$ar'^2_3 + br'_3 + c = 0 \quad (35)$$

where

$$a = h'_{3b}(2l_3 - b) + \frac{dh_1}{M_1} \quad (36)$$

$$b = 2h'_{3b}l_3(2b - 3l_3) - \frac{2l_3 dh_1}{M_1} \quad (37)$$

$$c = -4l_3^2 h'_{3b}(b - l_3) \quad (38)$$

with

$$d = l'_1 - l_1 + b \quad (39)$$

One solution will be negative and the other positive, but the correct solution will be positive.

In oculometric studies, the corneal radius of curvature, anterior chamber depth, and the height of Purkinje image PIII (in this case  $h'_{3b}$ ) are known. The position of the vertex of the equivalent mirror can be calculated, and the distance from the target to camera focus can be set to a known value.

The methods described above were used to calculate the anterior lens radius  $r'_3$ , and errors in the determination of  $r_3$  by the usual method of comparison phakometry based on Equation (1), calculated for both fixed and stationary targets for various target distances. The Gullstrand–Emsley schematic eye was used as the model to investigate these effects. Unit magnification was chosen for the height of Purkinje image PI and the height of Purkinje image PIII, determined by paraxial ray tracing, with the relationship between the two image heights given by Equation (7).

## Results

An example of a calculation of the anterior lens radius of curvature using these equations is given for each option, using the relevant values of the Gullstrand–Emsley schematic eye shown in *Table 1*.

### Option 1

If we assume a target distance  $s$  of 30 mm, and a normalised Purkinje image PI height  $h'_1$  of 1.000, then the relative height  $h'_3$  of Purkinje image PIII will be 1.828, distance  $w$  from the corneal vertex to the equivalent mirror will be 3.048 mm, and the calculation proceeds using Equations (10), (11), (13) and (15) to give:

$$\begin{array}{cccc} M_1 & l_3 & M_3 & r'_3 \\ 0.115 & -33.048 \text{ mm} & 0.2103 & 17.60 \text{ mm} \end{array}$$

The actual radius of curvature  $r_3$  can then be calculated as 11.00 mm as shown in the *Appendix*.

### Option 2

In this case if we assume that the distance from the target to the corneal vertex is 30.00 mm when the camera is focused on image PI, it will be 23.85 mm when the camera is focused on image PIII, and the distance  $t$  will be 33.45 mm. Again, if the height  $h'_1$  of Purkinje image PI is 1.000, the height  $h'_3$  of image PIII will be 2.143. These dimensions would usually be the measured values, but for

**Table 1.** The Gullstrand–Emsley schematic eye as proposed by Bennett and Rabbetts (1989)

Component	Symbol	Value
Radius of curvature		
Cornea	$r_1$	7.80
Lens (anterior)	$r_3$	11.00
Anterior chamber depth	$d_1$	3.60
Refractive index		
Aqueous	$n_2$	1.336
Lens	$n_3$	1.422

All dimensions in mm.

this example they have been calculated for the Gullstrand–Emsley eye. The calculation of  $r'_3$  can be made using Equations (18), (21), (23), (24) and (25):

$$\begin{array}{ccccc} M_1 & l_1 & l_3 & M_3 & r'_3 \\ 0.115 & -30 \text{ mm} & -28.835 \text{ mm} & 0.246 & 17.60 \text{ mm} \end{array}$$

Again, the actual radius  $r_3$  can be determined as shown in the *Appendix*.

### Option 3

Now consider a similar case to Option 1, where the target is 30 mm from the corneal vertex, the camera is focused on image PI, with a height  $h'_1$  of 1.00, and magnification  $M_1$  of 0.115. If the distance  $b$  from the entrance pupil of the camera to the target is assumed to be 200 mm then the defocused image of PIII will have a height of 1.778 when measured in the same plane as PI. From Equation (27), the image height  $h'_{3b}$  of 1.778 can be shown to correspond to the figure of 1.828 in Option 1, where the camera is focused on image PIII. This procedure can be simulated by using the Gullstrand–Emsley schematic eye, in which case we know  $r_1 = 7.80$  mm,  $w = 3.048$  mm, and if we assume  $l_1 = -30.00$  mm then  $l'_1 = 3.451$  mm. The distance  $l_3$  to the equivalent mirror will therefore be  $-33.048$  mm. The radius of curvature  $r'_3$  of the equivalent mirror can then be found from Equations (36) to (39) to be 17.60 mm, and the actual radius calculated as before.

The radius of curvature  $r_3$  obtained if no allowance was made for the target distance, or for refocusing of the camera with targets attached, i.e. using Equation (1), is shown in *Figure 4*. The difference between the true value

of 11.00 mm, and calculated value increases as the targets are placed closer to the eye, with a greater error if the targets are stationary (Option 1) and do not move when the camera is focused on image PIII, compared to a mobile target (Option 2). From *Figure 4*, the error in  $r'_3$  is less than 0.2 mm if the target distance is greater than about 300 mm for a stationary target and greater than 40 mm for a mobile target.

### Discussion

The methods described allow calculation of the radius of curvature of the anterior lenticular surface for various experimental arrangements, and obviate the need to collimate target sources that are placed at finite distances in front of the cornea in order to use conventional methods (Bennett and Rabbetts, 1989; Sorsby *et al.*, 1961) of calculation. One of the methods (Option 3) avoids the need to refocus the camera for recordings of Purkinje images PI and PIII. In the video phakometer described by Mutti *et al.* (1992) collimated targets were attached to the camera in order to overcome the errors from finite sources. However, there are advantages in having targets at finite distances in front of the cornea, the most important of which is that observation and recording of image PIII is facilitated. The quality of image PIII is notoriously poor, due in part to the nature of the anterior lens surface, but also to difficulties in correctly positioning the target and providing sufficient illuminance from the target to make the PIII image clearly visible. A target relatively close to the eye can improve the quality of this image, but leads to errors if the equivalent mirror is calculated in the usual manner. The use of a mobile target attached to the camera leads to smaller errors in calculating  $r_3$  from Equation (1) than a stationary target at all target distances. Provided mobile targets are at least 150 mm from the cornea, the errors in  $r_3$  based on the traditional method of calculation are quite small, whereas stationary targets would need to be at least 500 mm away to avoid significant errors. Our finding that the error in calculation of  $r_3$  by conventional methods is less for a given target distance if the target is attached to the camera is in agreement with Mutti *et al.* (1992) who calculated differences in lens power resulting from errors in both PIII and PIV. Errors in calculating  $r_3$  can therefore be avoided by collimating targets, using target distances that are greater than the figures given above, or using the computing scheme given in this paper.

We have addressed the problem of recording images in different planes in two ways. Options 1 and 2 allow for the camera to be moved from the plane containing images PI to the plane of image PIII, and Option 3 allows a single recording with correction of the height of defocused image PIII. Van Veen and Goss (1988) have suggested that an intermediate image plane may be used to obtain a 'best focus' for both images. The errors associated with this

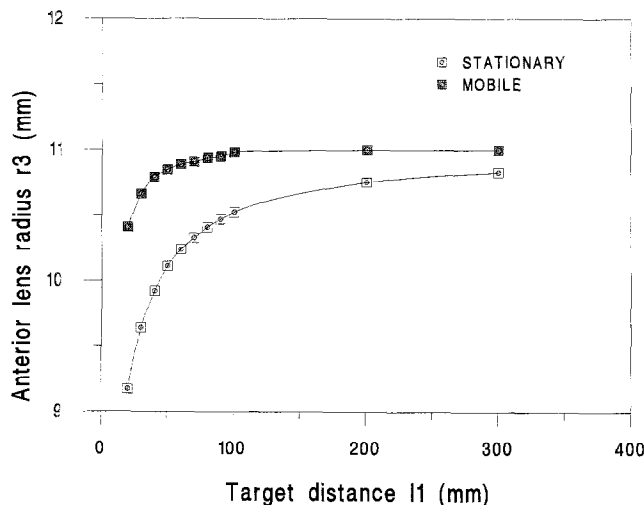


**Figure 4.** Anterior radius of curvature  $r_3$  calculated from Equation (1) for a stationary target (Option 1), and for a mobile target (Option 2). The difference between the Gullstrand–Emsley value of 11.00 mm and the calculated value is the error produced at each distance if no allowance is made for target distance  $l_1$ .

suggestion would depend on the target distances, and on the position of the entrance pupil of the camera.

The use of a telecentric stop to overcome the problems of images in different planes has been used by Philips *et al.* (1988). However this method may not be practical for use with standard video cameras because the application requires the aperture stop (diaphragm) to be moved from the usual position inside the lens, to a position coinciding with the back focal plane of the lens. Furthermore, the movement of the stop may lead to a change of aberrations, and because the stop must be placed close to the image plane the field of view could be severely reduced.

### Summary

A general method for calculating the radius of curvature of the anterior surface of the crystalline lens is derived, based on the radius of curvature of the equivalent mirror. The methods proposed allow for the target in conventional phakometry to be either attached to the camera, or mounted independently of the camera. The method also allows for either a single recording of the image heights PI and PIII to be made, in which the height of the defocused image PIII in the plane of PI can be calculated as a true image height, or for separate recordings to be made of PI and PIII. The error in calculation of the anterior lens radius of curvature by conventional methods is greater at finite target distances if the targets are fixed with respect to the eye under measurement, and do not move with the camera when focusing from image PI to PIII.

### Acknowledgement

The authors are grateful to Kerry King for his assistance with computer programming for this study.

### References

- Bennett, A. G. and Rabbetts, R. B. (1989). *Clinical Visual Optics* 2nd edn, Butterworth, London, UK, pp. 262, 477–478.
- Brown, N. (1973). The change in shape and internal form of the lens of the eye on accommodation. *Exp. Eye Res.* **15**, 441–459.
- Garner, L. F., Yap, M. K. H., Kinnear, R. F. and Frith, M. J. (1995). Ocular dimensions and refraction in Tibetan children. *Optom. Vision Sci.* **72**, 266–271.
- Mutti, D. O., Zadnik, K. and Adams, A. J. (1992). A video technique for phakometry of the crystalline lens. *Invest. Ophthalmol. Visual Sci.* **33**, 1771–1782.
- Philips, P., Perez-Emmanuelli, J., Rosskothien, H. D. and Koester, C. J. (1988). Measurement of intraocular lens decentration and tilt *in vivo*. *J. Cat. Refract. Surg.* **14**, 129–135.
- Sorsby, A., Benjamin, B. and Sheridan, M. (1961). Refraction and its components during the growth of the eye from the age of three. Medical Research Council, Special Report Series No. 310, London, HMSO, pp. 58–59.
- Van Veen, H. G. and Goss, D. A. (1988). Simplified system

for Purkinje image photography for phakometry. *Am. J. Optom. Vision Sci.* **65**, 905–908.

Zadnik, K., Mutti, D. O., Friedman, N. E. and Adams, A. J. (1993). Initial cross-sectional results from the Orinda longitudinal study of myopia. *Optom. Vision Sci.* **70**, 750–758.

### Appendix

The general paraxial equation,

$$\frac{n_2}{l'} - \frac{n_1}{l} = \frac{n_2 - n_1}{r} \quad (\text{A1})$$

can be written for refraction in the forms:

$$l' = \frac{n_2 l r}{[n_1 r + l(n_2 - n_1)]} \quad (\text{A2})$$

$$l = \frac{n_1 l' r}{[n_2 r - l'(n_2 - n_1)]} \quad (\text{A3})$$

or for reflection by substituting  $n_2 = -n_1$  to give:

$$l' = \frac{l r}{(2l - r)} \quad (\text{A4})$$

The radius of curvature  $r_3$  of the anterior lens can be found using the equivalent mirror theorem by finding the positions of the vertex and centre of curvature of the equivalent mirror.

From Equation (A2), given that the refractive index in object space is  $n_2$  and the refractive index in image space is  $n_1$ , we can find  $w$ , the distance from the image of the anterior surface of the lens to the corneal vertex:

$$w = \frac{n_1 d_1 r_1}{[n_2 r_1 + d_1(n_1 - n_2)]} \quad (\text{A5})$$

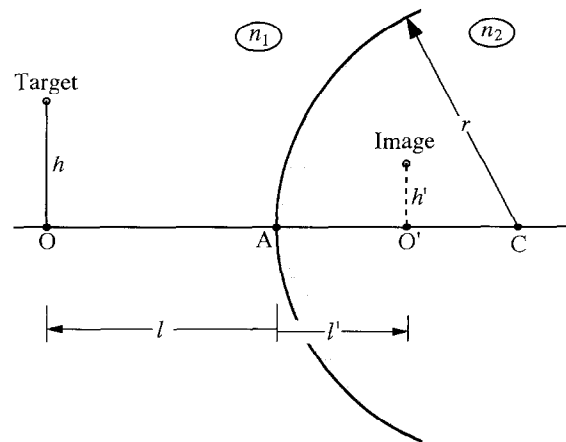


**Figure 5.** A spherical refracting surface of radius of curvature  $r$  forms an image at  $O'$  of an object at  $O$ .



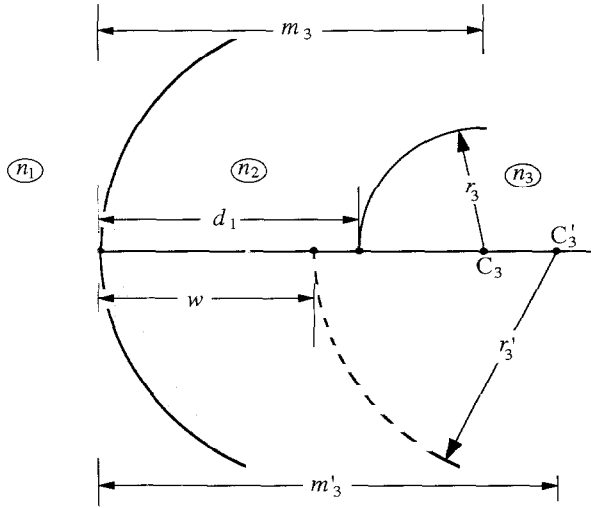


**Figure 6.** The radius of curvature  $r_3$  of the anterior lens surface, centre at  $C_3$  shown with respect to the equivalent mirror radius  $r'_3$ , centre  $C'_3$ .

The distance  $m'_3$  from the corneal vertex to the centre of curvature of the equivalent mirror is given by:

$$m'_3 = w + r'_3 \quad (\text{A6})$$

From Equation (A3), and given the same conditions for refractive index in image and object space, the position of the centre of curvature of the anterior lens surface with respect to the corneal vertex is:

$$m_3 = \frac{n_2 m'_3 r_1}{[n_1 r_1 + m'_3 (n_2 - n_1)]} \quad (\text{A7})$$

and  $r_3$ , the real radius of curvature, is given by:

$$r_3 = m_3 - d_1 \quad (\text{A8})$$